

On the Power of Gradual Network Alignment Using Dual-Perception Similarities

Jin-Duk Park, Cong Tran, Won-Yong Shin, *Senior Member, IEEE*, and Xin Cao, *Member, IEEE*

Abstract—Network alignment (NA) is the task of finding the correspondence of nodes between two networks based on the network structure and node attributes. Our study is motivated by the fact that, since most of existing NA methods have attempted to discover all node pairs *at once*, they do not harness information enriched through *interim* discovery of node correspondences to more accurately find the next correspondences during the node matching. To tackle this challenge, we propose Grad-Align, a new NA method that *gradually* discovers node pairs by making full use of node pairs exhibiting strong consistency, which are easy to be discovered in the early stage of gradual matching. Specifically, Grad-Align first generates node embeddings of the two networks based on graph neural networks along with our *layer-wise reconstruction loss*, a loss built upon capturing the first-order and higher-order neighborhood structures. Then, nodes are gradually aligned by computing *dual-perception similarity* measures including the *multi-layer embedding similarity* as well as the *Tversky similarity*, an asymmetric set similarity using the Tversky index applicable to networks with different scales. Additionally, we incorporate an edge augmentation module into Grad-Align to reinforce the structural consistency. Through comprehensive experiments using real-world and synthetic datasets, we empirically demonstrate that Grad-Align consistently outperforms state-of-the-art NA methods.

Index Terms—Consistency; dual-perception similarity; gradual network alignment; graph neural network; Tversky index

1 INTRODUCTION

1.1 Background and Motivation

MULTIPLE networks are ubiquitous in various real-world application domains, ranging from computer vision, bioinformatics, web mining, chemistry to social network analyses [1], [2]. Considerable attention has been paid to conducting network alignment (NA) (also known as graph matching), which is the task of finding the node correspondence across different networks and is often the very first step to perform downstream machine learning (ML) tasks on multiple networks in such applications, thus leading to more precise analyses. In social networks, the identification of different accounts (e.g., Facebook, Twitter, and Foursquare) of the same user facilitates friend recommendation, user behavior prediction, and personalized advertisement [1], [2], [3]. For example, by discovering the correspondence between Twitter and Foursquare networks of the same user, we can improve the performance of friend/location recommendations for Foursquare users whose social connections and activities can be very sparse

[4]. As another example, in bioinformatics, aligning tissue-specific protein-protein interaction (PPI) networks can be effective in solving the problem of candidate gene prioritization [5].

Despite the effectiveness and utilities of NA, performing the NA task poses several practical challenges. First, a fundamental assumption behind existing NA methods is the structural and/or attribute *consistencies*. That is, the same node is assumed to have a consistency over its connectivity structure and/or its metadata (i.e., attributes) across different networks [1]. However, such consistency constraints are not often satisfied in real-world applications. Examples of structural consistency violations include but are not limited to the following cases: 1) a user might have more connections in one social network site (e.g., Facebook) than those in another site (e.g., LinkedIn) and 2) the same gene might exhibit considerably different interaction patterns across different tissue-specific PPI networks [1], [5]. Moreover, there exist users who deliberately use different usernames across multiple social networks [6], which violates the assumption of attribute consistency. Thus, not all ground truth cross-network node pairs are always *strongly consistent*. Our study is basically initiated by the fact that most of existing NA methods (e.g., [1], [3], [7], [8], [9], [10]) have attempted to discover all node pairs *at once* based on modeling their own similarity between cross-network node pairs (refer to Fig. 1), which thereby may not take advantage of the information enriched through *interim* discovery of node pairs in order to more accurately find the next node pairs during the node matching. The motivation of our study is that strongly consistent node pairs, which are easy to be found, can be very informative when discovering node pairs having weak consistency; how to exploit the information of the strongly consistent node pairs remains a technical challenge in the

- Jin-Duk Park is with the School of Mathematics and Computing (Computational Science and Engineering), Yonsei University, Seoul 03722, South Korea.
E-mail: jindeok6@yonsei.ac.kr
- Cong Tran is with the Faculty of Information Technology, Posts and Telecommunications Institute of Technology, Hanoi 100000, Vietnam.
E-mail: congtr@ptit.edu.vn
- Won-Yong Shin is with the School of Mathematics and Computing (Computational Science and Engineering), Yonsei University, Seoul 03722, South Korea, and the Graduate School of Artificial Intelligence, Pohang University of Science and Technology (POSTECH), Pohang 37673, South Korea.
E-mail: wy.shin@yonsei.ac.kr
- Xin Cao is with the School of Computer Science and Engineering, The University of New South Wales, Sydney 2052, Australia.
E-mail: xin.cao@unsw.edu.au
(Corresponding author: Won-Yong Shin.)

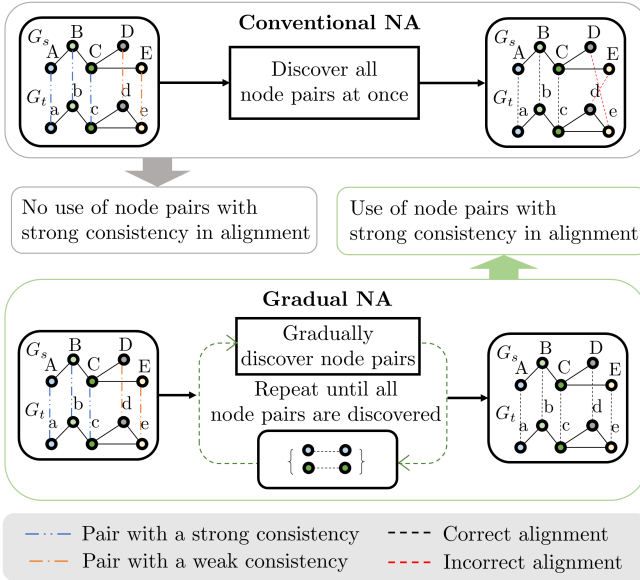


Fig. 1: Comparison of conventional NA methods and our Grad-Align method.

NA task.

Second, more importantly, source and target networks often manifest *different scales* in terms of the number of nodes. The NA task has been carried out using benchmark datasets consisting of two imbalanced networks (see [1], [2], [3], [6], [8], and references therein)—for example, the Douban Online and Douban Offline networks have 3,906 and 1,118 users, respectively [11]. Unfortunately, the problem raised by such networks with different scales exacerbates the inconsistency of cross-network node pairs, which thus results in a low alignment accuracy. It is another open challenge how to overcome this network imbalance problem in conducting NA.

Motivated by the above-mentioned open challenges, we push forward the state-of-the-art performance by designing a new NA method that universally shows the superior performance even including the case of networks with different scales.

1.2 Main Contributions

In this paper, we introduce Grad-Align, a novel NA method that *gradually* finds the node correspondence.¹ Grad-Align discovers only a part of node pairs iteratively until all node pairs are found in order to combat the node inconsistency across two different networks, while fully exploiting the information of already aligned node pairs having strong consistency and/or the prior matching information in discovering weakly consistent node pairs.

To this end, we characterize and compute our own similarity measure between nodes across two networks, termed the *dual-perception similarity*, which is composed of the *multi-layer embedding similarity* and the *Tversky similarity*. We first calculate the similarity of multi-layer embeddings

1. The source code used in this paper is available online (<https://github.com/jindeok/Grad-Align-full>).

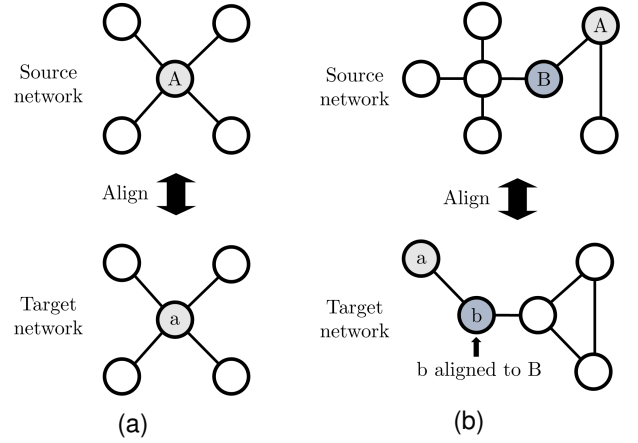


Fig. 2: An example illustrating a node pair (A,a) that reveals (a) strong structural consistency and (b) weak structural consistency.

using graph neural networks (GNNs), where the weight-sharing technique is used to consistently generate hidden representations for each network and a newly designed layer-wise reconstruction loss is used to precisely capture multi-hop neighborhood structures during training. Then, we calculate the Tversky similarity, which is a newly devised asymmetric set similarity measure using the Tversky index [12] to alleviate the problem of network scale imbalance. By iteratively updating our dual-perception similarity, we gradually match a part of node pairs until all node correspondences are found.

For a better understanding, we give an instance of two different networks including a node pair with either strong or weak structural consistency in Fig. 2, which intuitively explains why gradually discovering node pairs is beneficial. Suppose that nodes A and B in a source network correspond to nodes a and b in a target network, respectively, as the ground truth mapping. Since a cross-network node pair (A, a) in Fig. 2a has strong structural consistency, it can be easily discovered. On the contrary, it is difficult to discover a node pair (A, a) in Fig. 2b due to its weak structural consistency. In this case, exploiting the information of already aligned node pairs that potentially exhibit strong consistency can be quite useful in discovering weakly consistent node pairs. For example, when we are aware of the node correspondence (B, b) beforehand through gradual matching, it would be much easier to discover the node pair (A, a) due to the fact that nodes A and a are direct neighbors of nodes B and b, respectively. Thus, we are capable of more effectively and precisely finding the node correspondence across different networks via such gradual matching.

The proposed design methodology is built upon rigorous theoretical frameworks by proving that 1) the weight-sharing technique in GNNs guarantees the consistency of cross-network nodes in the embedding space and 2) the impact and benefits of the Tversky similarity are higher than those of the well-known Jaccard index in terms of the growth rate of each similarity measure. Additionally, we analyze the computational complexity of our Grad-Align method. To further improve the performance of Grad-Align

by strengthening the structural consistency, we also show its reinforced version that incorporates edge augmentation into the Grad-Align method.

To validate the superiority of our Grad-Align method, we comprehensively perform empirical evaluations using various real-world and synthetic datasets. Experimental results show that our method consistently outperforms state-of-the-art NA methods regardless of the datasets while showing substantial gains up to 75.54% compared with the second-best performer. We also scrutinize the impact of each module in Grad-Align via ablation studies. Moreover, our experimental results demonstrate the robustness of our Grad-Align method to both structural and attribute noises owing to our dual-perception similarity.

The main technical contributions of this paper are five-fold and summarized as follows:

- We introduce Grad-Align, a novel NA method that gradually finds the node correspondence;
- We characterize the dual-perception similarity to better capture the consistency of nodes across networks;
- We formulate the Tversky similarity applicable to networks with different scales;
- We validate the performance of Grad-Align through extensive experiments using real-world datasets as well as synthetic datasets;
- We further introduce Grad-Align-EA, a variant of the original Grad-Align method to reinforce the structural consistency across networks.

1.3 Organization and Notations

The remainder of this paper is organized as follows. In Section 2, we present prior studies that are related to NA. In Section 3, we explain the methodology of our study, including the problem definition and an overview of our Grad-Align method. Section 4 describes technical details of the proposed method. Comprehensive experimental results are shown in Section 5. Finally, we provide a summary and concluding remarks in Section 6.

Table 1 summarizes the notation that is used in this paper. This notation will be formally defined in the following sections when we introduce our methodology and the technical details.

2 RELATED WORK

The method that we propose in this paper is related to three broader fields of research, namely NA only with topological information, NA with attribute information, and network embedding-aided NA.

NA only with topological information. The topological similarity of networks is a basic and core feature to identify the node correspondence between two given networks. Specifically, given the topological structure of two networks, IsoRank [9] was designed by propagating the pairwise node similarity and structural consistency to discover the node correspondence. NetAlign [10] formulated the NA problem as an integer quadratic program. CLF [13] presented collective link fusion across partially aligned probabilistic networks. Moreover, BIG-ALIGN [14] was developed by using the alternating projected gradient descent approach

Notation	Description
G_s	Source network
\mathcal{V}_s	Set of nodes in G_s
\mathcal{E}_s	Set of edges in G_s
\mathcal{X}_s	Set of attributes of nodes in \mathcal{V}_s
G_t	Target network
\mathcal{V}_t	Set of nodes in G_t
\mathcal{E}_t	Set of edges in G_t
\mathcal{X}_t	Set of attributes of nodes in \mathcal{V}_t
n_s	Number of nodes in G_s
n_t	Number of nodes in G_t
$\pi^{(i)}$	One-to-one node mapping at the i -th iteration
M	Total number of ground truth node pairs
$\tilde{\mathcal{V}}_s^{(i)}$	Set of seed nodes in G_s up to the i -th iteration
$\tilde{\mathcal{V}}_t^{(i)}$	Set of seed nodes in G_t up to the i -th iteration
$\hat{\mathcal{V}}_s^{(i)}$	Set of newly aligned nodes in G_s at the i -th iteration
$\hat{\mathcal{V}}_t^{(i)}$	Set of newly aligned nodes in G_t at the i -th iteration
$\tilde{\mathcal{V}}_s^{(0)}$	Set of prior seed nodes in G_s
$\tilde{\mathcal{V}}_t^{(0)}$	Set of prior seed nodes in G_t
$\mathbf{H}_s^{(l)}$	Hidden representation in G_s at the l -th GNN layer
$\mathbf{H}_t^{(l)}$	Hidden representation in G_t at the l -th GNN layer
\mathbf{S}_{emb}	Multi-layer embedding similarity matrix
$\mathbf{S}^{(i)}$	Tversky similarity matrix at the i -th iteration
$\mathbf{S}^{Tve(i)}$	Dual-perception similarity matrix at the i -th iteration

TABLE 1: Summary of notations.

that aims at solving a constrained optimization problem while finding permutation matrices in NA.

NA with attribute information. In addition to the structural information, node attributes are another distinguishable feature that helps us find the node correspondence. For example, the profile attributes of each user such as the name, affiliation, and description can be valuable for aligning the same user across social networks [15]. REGAL [8] was presented by performing a low-rank implicit approximation of a similarity matrix that incorporates the structural similarity and attribute agreement between nodes in two disjoint graphs. ULink [16] was proposed by exploring the concept of latent userspace to more naturally model the relationship between the underlying real users. FINAL [1] was presented by leveraging not only the node attribute information but also the edge attribute information in the topology-based NA process.

Network embedding-aided NA. With the increasing attention to network embedding (also known as network representation learning) and its diverse applications in solving downstream ML problems, network embedding-aided NA has recently become in the spotlight. Network embedding learns a mapping from each node in a graph to a low-dimensional vector in an embedding space while preserving intrinsic network properties (e.g., the neighborhood structure and high-order proximities), thus resulting in an efficient and scalable representation of the underlying graph [17]. PALE [7] was presented by exploiting the first-order and second-order proximities of node pairs in the embedding space and further adopting a multi-layer perceptron (MLP) architecture to capture the nonlinear relationship between the resulting network embeddings from two different networks. DeepLink [3] was presented by employing an unbiased random walk to generate node embeddings of two given networks based on the Skip-gram model [18] and

using an autoencoder as a mapping function to discover the relation between two embeddings. IONE [6] was designed for solving the NA problem by learning an aligned network embedding in multiple directed and weighted networks. CENALP [19] was presented by jointly performing NA and link prediction tasks to enhance the alignment accuracy, where a cross-graph embedding method based on random walks was devised. In [19], the structural and node attribute similarities were taken into account to predict cross-network links. Moreover, since GNNs [20], [21], [22], [23] have emerged as a powerful network feature extractor in attributed networks, GAlign [2] was developed by making use of the multi-order (multi-layer) nature of graph convolutional network (GCN) [20] for NA.

Discussion. Although the aforementioned NA approaches achieve convincing alignment performance under their own network settings, they pose several practical challenges. Precisely, the methods were inherently designed in such a way that their performance depend highly on either the topological information [3], [9], [13], [14] or the attribute information [1], [2], [8]; such a high dependency makes the designed model vulnerable to topological or attribute inconsistency across networks. Moreover, most of the conventional methods such as [3], [8], [9], [13], [14], [24] find all node pairs *at once* without leveraging already discovered node pairs during the node matching, which often fails to correctly find the correspondence of nodes exhibiting weak consistency. Although there was an attempt to find node pairs iteratively (see [19]), the method focuses on performing NA along with link prediction to enrich the structure information by newly added links. Thus, the impact and benefits of gradual alignment in improving the alignment accuracy were underexplored yet.

3 METHODOLOGY

In this section, as a basis for the proposed Grad-Align method in Section 4, we first describe our network model with basic assumptions and formulate the NA problem. Then, we explain an overview of our Grad-Align method using dual-perception similarity measures as a solution to the problem.

3.1 Network Model and Basic Assumptions

We assume source and target networks to be aligned, denoted as G_s and G_t , respectively. For simplicity, we assume both G_s and G_t to be undirected and unweighted networks without self-loop or repeated edges. For the source network $G_s = (\mathcal{V}_s, \mathcal{E}_s, \mathcal{X}_s)$, \mathcal{V}_s is the set of nodes (or equivalently, vertices) in G_s whose size is n_s (i.e., $|\mathcal{V}_s| = n_s$); \mathcal{E}_s is the set of edges between pairs of nodes in \mathcal{V}_s ; and $\mathcal{X}_s \in \mathbb{R}^{n_s \times d}$ is the set of node attribute (feature) vectors, where d is the number of attributes per node. For the target network $G_t = (\mathcal{V}_t, \mathcal{E}_t, \mathcal{X}_t)$, notations \mathcal{V}_t , \mathcal{E}_t , and \mathcal{X}_t similarly follow those in G_s with $|\mathcal{V}_t| = n_t$ and $\mathcal{X}_t \in \mathbb{R}^{n_t \times d}$.² In our study, we assume that there are M ground truth cross-network node pairs to be discovered.

2. Here, the number of node attributes for both networks is assumed to be the same as in other NA methods (see [1], [2], [19]).

3.2 Problem Definition

In the following, we formally define the NA problem for given two networks G_s and G_t as follows.

Definition 3.1 (NA). *Given two networks $G_s = (\mathcal{V}_s, \mathcal{E}_s, \mathcal{X}_s)$ and $G_t = (\mathcal{V}_t, \mathcal{E}_t, \mathcal{X}_t)$, NA aims to find one-to-one mapping $\pi : \mathcal{V}_s \rightarrow \mathcal{V}_t$, where $\pi(u) = v$ and $\pi^{-1}(v) = u$ for $u \in \mathcal{V}_s$ and $v \in \mathcal{V}_t$.*

3.3 Overview of Grad-Align

In this subsection, we describe the overview of our Grad-Align method using the *dual-perception* similarity. We start by stating that the standard protocol of NA involves the computation of the similarity between cross-network node pairs, followed by the utilization of assignment algorithms to discover cross-network node pairs from the similarity matrix [1], [2], [8], [25]. Our method basically follows the standard protocol of NA but attempts to gradually discover cross-network node pairs based on two different types of similarity measures, including 1) the similarity of *multi-layer* embeddings and 2) the *Tversky similarity* as a newly characterized asymmetric set similarity using the Tversky index [12]. First, to generate multi-layer embeddings, GNNs are adopted for effectiveness in representing the structural and attribute semantic relations between nodes. Second, the Tversky similarity enables us to overcome the problem raised by networks with different scales. As illustrated in Fig. 3, our Grad-Align is basically composed of three main phases: 1) the multi-layer embedding similarity calculation, 2) the Tversky similarity calculation, and 3) the gradual node matching.

(Phase 1) We first focus on calculating the *multi-layer* embedding similarity matrix via L -layer GNN. Let $\mathbf{H}_s^{(l)} \in \mathbb{R}^{n_s \times h}$ and $\mathbf{H}_t^{(l)} \in \mathbb{R}^{n_t \times h}$ denote the hidden representation in G_s and G_t , respectively, at the l -th GNN layer where $l \in \{1, \dots, L\}$ and h is the dimension of each representation vector. As illustrated in Fig. 3, in the feed-forward process of GNN, we use the weight-sharing technique in order to consistently generate $\mathbf{H}_s^{(l)}$ and $\mathbf{H}_t^{(l)}$ at each layer. We then train the generated GNN model parameters via a *layer-wise reconstruction loss* to make each node representation more distinguishable by exploiting the nodes' proximities up to the l -th order (which will be specified in Section 4.1). Using the hidden representations $\mathbf{H}_s^{(l)}$ and $\mathbf{H}_t^{(l)}$ at each layer through training iterations, we are capable of computing the multi-layer embedding similarity matrix $\mathbf{S}_{emb} \in \mathbb{R}^{n_s \times n_t}$, which is expressed as

$$\mathbf{S}_{emb} = \sum_l \mathbf{H}_s^{(l)} \mathbf{H}_t^{(l)\top}, \quad (1)$$

where the superscript \top denotes the transpose of a matrix and each entry in \mathbf{S}_{emb} represents the similarity of pairwise node embedding vectors in the two networks G_s and G_t .

(Phase 2) We turn to calculating the Tversky similarity matrix. We start by denoting the set of one-hop neighbors of node u in G_s and the set of one-hop neighbors of node v in G_t as $\mathcal{N}_{G_s, u}$ and $\mathcal{N}_{G_t, v}$, respectively. Since the Tversky similarity calculation runs iteratively, we define $\pi^{(i)}$ as the mapping function at the i -th iteration. To characterize our

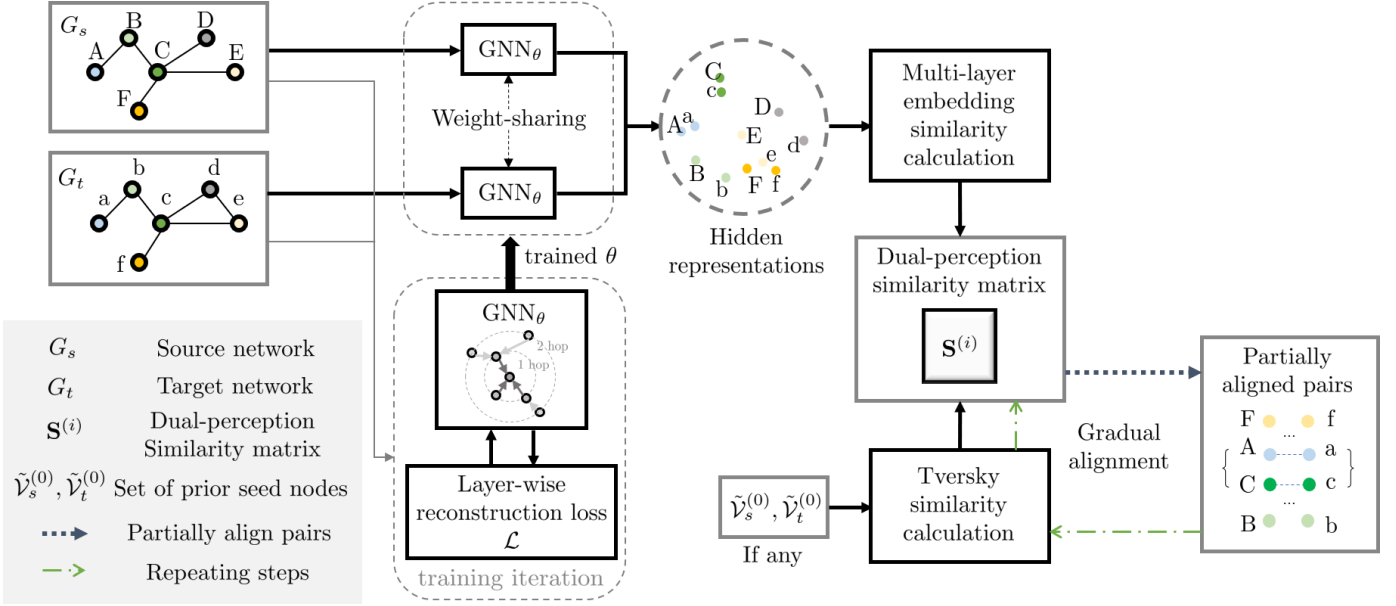


Fig. 3: The schematic overview of our Grad-Align method.

new similarity, we also define the ‘‘aligned cross-network neighbor-pair (ACN)’’ as follows.

Definition 3.2. (ACN). Given a node pair (u, v) , if $x \in \mathcal{N}_{G_s, u}$, $y \in \mathcal{N}_{G_t, v}$, and $\pi^{(i)}(x) = y$ (i.e., (x, y) is the already aligned node pair), then the node pair (x, y) belongs an ACN of (u, v) across two networks.

Then, for each iteration, we are interested in counting the number of ACNs of node pair (u, v) , i.e., the intersection of the two sets $\mathcal{N}_{G_s, u}$ and $\mathcal{N}_{G_t, v}$, indicating one-hop neighbors of nodes $u \in \mathcal{V}_s$ and $v \in \mathcal{V}_t$, respectively, upon the one-to-one node mapping $\pi^{(i)}$. However, there is a practical challenge on measuring ACNs. In particular, since two networks are often severely imbalanced in terms of the number of nodes, the most well-known set similarity measure, referred to as the Jaccard index, fails to precisely capture what portion of ACNs are shared. To remedy this problem, we present the Tversky similarity as an asymmetric set similarity measure using the Tversky index. We compute the Tversky similarity matrix $\mathbf{S}_{Tve}^{(i)} \in \mathbb{R}^{n_s \times n_t}$ iteratively by balancing between the set differences of two sets. The detailed description of $\mathbf{S}_{Tve}^{(i)}$ will be shown in Section 4. Finally, we calculate our proposed similarity matrix $\mathbf{S}^{(i)} \in \mathbb{R}^{n_s \times n_t}$, namely the dual-perception similarity matrix, at each iteration using the two similarity matrices as follows:

$$\mathbf{S}^{(i)} = \mathbf{S}_{emb} \odot \mathbf{S}_{Tve}^{(i)}, \quad (2)$$

where \odot indicates the element-wise matrix multiplication operator.

(Phase 3) We explain how to gradually match node pairs using our dual-perception similarity $\mathbf{S}^{(i)}$ in (2) for each iteration. Since \mathbf{S}_{emb} does not change over iterations, we focus only on how to update the Tversky similarity $\mathbf{S}_{Tve}^{(i)}$. From the fact that the NA problem is often solved under the supervision of some observed anchor nodes [1], [2], [7], we suppose that there are two sets of *prior seed nodes* (also known as anchor nodes) in two different networks, denoted

by $\tilde{\mathcal{V}}_s^{(0)}$ and $\tilde{\mathcal{V}}_t^{(0)}$ in source and target networks, respectively, whose links connecting them correspond to the ground truth prior anchor information for NA. These two sets are utilized to *initially* calculate $\mathbf{S}_{Tve}^{(1)}$ along with the node mapping function $\pi^{(0)}$.³ By iteratively updating $\mathbf{S}_{Tve}^{(i)}$ based on the information of newly aligned node pairs, Grad-Align makes full use of node pairs exhibiting strong consistency as well as prior seed node pairs (i.e., pairs that connect $\tilde{\mathcal{V}}_s^{(0)}$ and $\tilde{\mathcal{V}}_t^{(0)}$). Next, we explain our gradual alignment process. Let $\tilde{\mathcal{V}}_s^{(i)}$ and $\tilde{\mathcal{V}}_t^{(i)}$ denote the set of aligned nodes in G_s and G_t , respectively, up to the i -th iteration. Then, it follows that $\tilde{\mathcal{V}}_s^{(i)} = \tilde{\mathcal{V}}_s^{(i-1)} \cup \hat{\mathcal{V}}_s^{(i)}$, where the subscript $*$ represents s and t for source and target networks, respectively, and $\hat{\mathcal{V}}_s^{(i)}$ is the set of *newly* aligned nodes in each network at the i -th iteration. By iteratively calculating the dual-perception similarity matrix $\mathbf{S}^{(i)}$ in (2), we discover $|\hat{\mathcal{V}}_s^{(i)}| = |\hat{\mathcal{V}}_t^{(i)}| = N$ cross-network node pairs at each iteration, where $|\cdot|$ is the cardinality of the set, and $N > 0$ is a positive integer. To this end, similarly as in [1], [19], we employ a ranking-based selection strategy that selects the top- N elements in the matrix $\mathbf{S}^{(i)}$ for each iteration (which will be specified in Section 4.1). Then, since the node mapping $\pi^{(i)}$ is updated to $\pi^{(i+1)}$ after N node pairs are newly found, the matrix $\mathbf{S}_{Tve}^{(i+1)}$ is recalculated accordingly in order to update $\pi^{(i+2)}$. The process is repeated until all node correspondences (i.e., M node pairs) are found. Specifically, the iteration ends when i becomes $\lceil \frac{M}{N} \rceil + 1$, where $\lceil \cdot \rceil$ is the ceiling operator.⁴

The schematic overview of our Grad-Align is presented in Fig. 3. The two most consistent pairs (A, a) and (C, c) are aligned at the first step as the similarities of (A, a) and (C, c) in $\mathbf{S}^{(1)}$ are higher than those of other cross-network node pairs.

3. If $\tilde{\mathcal{V}}_s^{(0)}$ and $\tilde{\mathcal{V}}_t^{(0)}$ are \emptyset , which means that no prior information is given, then we only use \mathbf{S}_{emb} at the first matching step.

4. Note that the number of node pairs to be aligned at the last iteration may be less than N .

Algorithm 1 : Grad-Align

Input: $G_s, G_t, \tilde{\mathcal{V}}_s^{(0)}, \tilde{\mathcal{V}}_t^{(0)}$
Output: $\pi_{(\lceil \frac{M}{N} \rceil + 1)}$

- 1: **Initialization:** $\theta \leftarrow$ random initialization; $i \leftarrow 1$
- 2: /* Calculation of \mathbf{S}_{emb} */
- 3: **while** not converged **do**
- 4: $\mathbf{H}_s^{(1)}, \mathbf{H}_s^{(2)}, \dots, \mathbf{H}_s^{(L)} \leftarrow \text{GNN}_\theta(G_s)$
- 5: $\mathbf{H}_t^{(1)}, \mathbf{H}_t^{(2)}, \dots, \mathbf{H}_t^{(L)} \leftarrow \text{GNN}_\theta(G_t)$
- 6: $\mathcal{L} \leftarrow$ layer-wise reconstruction loss in (8)
- 7: Update θ by taking one step of gradient descent
- 8: **end while**
- 9: $\mathbf{S}_{emb} \leftarrow \sum_{l=1}^L \mathbf{H}_s^{(l)} \mathbf{H}_t^{(l)\top}$
- 10: /* Gradual matching by updating $\mathbf{S}_{Tve}^{(i)}$ */
- 11: **if** $\tilde{\mathcal{V}}_s^{(0)} = \tilde{\mathcal{V}}_t^{(0)} = \emptyset$ **then**
- 12: $\mathbf{S}^{(i)} \leftarrow \mathbf{S}_{emb}$
- 13: **else**
- 14: Calculate $\mathbf{S}_{Tve}^{(i)}$ using (9)
- 15: $\mathbf{S}^{(i)} \leftarrow \mathbf{S}_{emb} \odot \mathbf{S}_{Tve}^{(i)}$
- 16: **end if**
- 17: **while** $i \leq \lceil \frac{M}{N} \rceil$ **do**
- 18: Find $\hat{\mathcal{V}}_s^{(i)}$ and $\hat{\mathcal{V}}_t^{(i)}$ based on $\mathbf{S}^{(i)}$
- 19: $i \leftarrow i + 1$
- 20: Update mapping $\pi^{(i)}$:
 $\{\pi^{(i)}(u) = v \mid u \in \hat{\mathcal{V}}_s^{(i-1)}, v \in \hat{\mathcal{V}}_t^{(i-1)}\}$
- 21: Update $\mathbf{S}_{Tve}^{(i)}$ using (9)
- 22: $\mathbf{S}^{(i)} \leftarrow \mathbf{S}_{emb} \odot \mathbf{S}_{Tve}^{(i)}$
- 23: **end while**
- 24: **return** $\pi_{(\lceil \frac{M}{N} \rceil + 1)}$

4 PROPOSED GRAD-ALIGN METHOD

In this section, we elaborate on our Grad-Align method that gradually discovers the node correspondence using dual-perception similarities. We also analyze the computational complexity of Grad-Align. Furthermore, we present an enhanced version of Grad-Align, namely Grad-Align-EA, that incorporates the edge augmentation module into the original method.

4.1 Methodological Details of Grad-Align

We start by recalling that Grad-Align consists of three key phases, including 1) the multi-layer embedding similarity calculation, 2) the Tversky similarity calculation, and 3) the gradual node matching. The overall procedure of the proposed Grad-Align method is summarized in Algorithm 1, where θ and GNN_θ indicate the trainable model parameters and the GNN model parameterized by θ .

First, let us describe how to calculate the multi-layer embedding similarity matrix \mathbf{S}_{emb} using a GNN model. Since our Grad-Align method is *GNN-model-agnostic*, we show a general form of the message passing mechanism [21], [22], [26] of GNNs in which we repeatedly update the representation of each node by aggregating representations of its neighbors using two functions, namely AGGREGATE and UPDATE. Formally, at the l -th hidden layer of a GNNs, AGGREGATE_u^l aggregates (latent) feature information from

the local neighborhood of node u in a given graph as follows:

$$\mathbf{m}_u^l \leftarrow \text{AGGREGATE}_u^l(\{\mathbf{h}_{x_u}^{l-1} \mid x_u \in \mathcal{N}_u \cup u\}, \mathbf{W}_1^l), \quad (3)$$

where $\mathbf{h}_{x_u}^{l-1} \in \mathbb{R}^{1 \times h}$ denotes the h -dimensional latent representation vector of node x_u at the $(l-1)$ -th hidden layer; \mathcal{N}_u indicates the set of neighbor nodes of u ; $\mathbf{W}_1^l \in \mathbb{R}^{h \times h}$ is the learnable weight matrix at the l -th layer for the AGGREGATE step; and \mathbf{m}_u^l is the aggregated information at the l -th layer. Here, \mathbf{h}_u^0 represents the node attribute vector of node u . In the UPDATE step, the latent representation at the next hidden layer is updated by using each node and its aggregated information from AGGREGATE_u^l as follows:

$$\mathbf{h}_u^l \leftarrow \text{UPDATE}_u^l(u, \mathbf{m}_u^l, \mathbf{W}_2^l), \quad (4)$$

where $\mathbf{W}_2^l \in \mathbb{R}^{h^m \times h^l}$ is the learnable weight matrix at the l -th layer for the UPDATE step.⁵ The above two functions AGGREGATE and UPDATE in (3) and (4), respectively, can be specified by several milestone GNN models such as GCN [20], GraphSAGE [21], and GIN [22]. Meanwhile, there is a practical challenge on implementing GNN model architectures aimed at performing the NA task. Specifically, since most of existing GNN models are not originally designed for learning node representations in multiple networks, a direct application of GNNs to the two networks G_s and G_t may not generate desirable node embeddings along with structural and attribute consistencies of nodes [2]. In other words, while a pair of nodes across two networks has the same neighborhood structure and/or attribute information, their representations may fail to be mapped closely together into the embedding space. To solve this problem, we employ the technique of sharing weight matrices between two GNN models for G_s and G_t (refer to lines 4–5 in Algorithm 1). We would like to establish the following proposition, which states that the weight-sharing technique in GNNs naturally supports the consistency of cross-network nodes in the embedding space in the context of NA.

Proposition 4.1. *Suppose that two networks G_s and G_t are isomorphic,⁶ where any of node pairs (u, v) matched by ground truth node mapping $\pi : \mathcal{V}_s \rightarrow \mathcal{V}_t$ have the same node attributes $\mathbf{h}_u^0 = \mathbf{h}_v^0$. Given two GNN models for G_s and G_t , if the weight matrices $\{\mathbf{W}_1^p\}_{p=1, \dots, L}$ and $\{\mathbf{W}_2^p\}_{p=1, \dots, L}$ are shared, then it follows that $\mathbf{h}_u^p = \mathbf{h}_v^p$ for all positive integers p , where L indicates the number of GNN layers.*

Proof. We prove this proposition by the mathematical induction for all layers $p = 1, \dots, L$, where $p = 1$ and $p > 2$ correspond to the base step and the consecutive inductive steps, respectively.

Base step: For node $u \in \mathcal{V}_s$, it follows that

$$\begin{aligned} \mathbf{m}_u^1 &\leftarrow \text{AGGREGATE}_u^1(\{\mathbf{h}_x^0 \mid x \in \mathcal{N}_u \cup u\}, \mathbf{W}_1^1) \\ \mathbf{h}_u^1 &\leftarrow \text{UPDATE}_u^1(u, \mathbf{m}_u^1, \mathbf{W}_2^1). \end{aligned} \quad (5)$$

For node $v \in \mathcal{V}_t$, we have

$$\begin{aligned} \mathbf{m}_v^1 &\leftarrow \text{AGGREGATE}_v^1(\{\mathbf{h}_y^0 \mid y \in \mathcal{N}_v \cup v\}, \mathbf{W}_1^1) \\ \mathbf{h}_v^1 &\leftarrow \text{UPDATE}_v^1(v, \mathbf{m}_v^1, \mathbf{W}_2^1). \end{aligned} \quad (6)$$

⁵ Note that the two learnable weight matrices \mathbf{W}_1^l and \mathbf{W}_2^l can be excluded depending on a specific choice of GNNs.

⁶ Two networks G_s and G_t are isomorphic when there exists a function $f : \mathcal{V}_s \rightarrow \mathcal{V}_t$ such that any two nodes u_1 and u_2 of \mathcal{V}_s are adjacent in G_s if and only if $f(u_1)$ and $f(u_2)$ are adjacent in G_t [27].

From (5) and (6), the equality $\{\mathbf{h}_x^0 | x \in \mathcal{N}_u \cup u\} = \{\mathbf{h}_y^0 | y \in \mathcal{N}_v \cup v\}$ is met due to the assumptions that G_s and G_t are isomorphic and $\mathbf{h}_u^0 = \mathbf{h}_v^0$, thus resulting in $\mathbf{m}_u^1 = \mathbf{m}_v^1$ from the AGGREGATE function. Using the UPDATE function finally yields $\mathbf{h}_u^1 = \mathbf{h}_v^1$.

Inductive step: Suppose that

$$\mathbf{h}_u^p = \mathbf{h}_v^p \quad (7)$$

for $p = k$, where $k \in \{1, \dots, L-1\}$. Then, it is not difficult to show that (7) also holds for $p = k+1$ using (3) and (4), which completes the proof of this proposition. \square

Now, we describe how to train GNN model parameters θ . Unlike prior studies including [3], [7], which utilized supervision data to learn the relationship between distinct latent spaces, we use the weight-sharing technique in GNNs that inherently supports the node consistency across two different networks in the embedding space (refer to Proposition 4.1). Thus, in our study, we train the parameters of GNNs unsupervisedly, similarly as in [2]. From the fact that the hidden representation at the l -th GNN layer contains the collective information of up to l -hop neighbors of nodes [20], [21], [28], [29], we make use of the adjacency matrix and its powers up to order l along with the l -th layer hidden representation. To this end, we present our new *layer-wise reconstruction loss* function for training the GNN model as follows (refer to line 6):

$$\mathcal{L} = \sum_{* \in \{s,t\}} \sum_l \left\| \tilde{D}_*^{(l)-\frac{1}{2}} \tilde{A}_*^{(l)} \tilde{D}_*^{(l)-\frac{1}{2}} - H_*^{(l)} H_*^{(l)\top} \right\|_F, \quad (8)$$

where the subscript $*$ represents s and t for source and target networks, respectively; $\tilde{A}_*^{(l)} = \sum_{k=1}^l \hat{A}_*^k$ where $\hat{A}_* = A_* + I_*$ is the adjacency matrix with self-connections in which I_* is the identity matrix; $\tilde{D}_*^{(l)}$ is a diagonal matrix whose (i, i) -th element is $\tilde{D}_*^{(l)}(i, i) = \sum_j \tilde{A}_*^{(l)}(i, j)$ where $\tilde{A}_*^{(l)}(i, j)$ is the (i, j) -th element of $\tilde{A}_*^{(l)}$; and $\|\cdot\|_F$ is the Frobenius norm of a matrix. By training the GNN model via our layer-wise reconstruction loss in (8), we are capable of precisely capturing the first-order and higher-order neighborhood structures. Note that, unlike the prior study (e.g., [2]), we use the *aggregated* matrix $\tilde{A}_*^{(l)}$ to reconstruct the underlying network from each hidden representation.

Next, we turn to explaining how to calculate the Tversky similarity matrix $\mathbf{S}_{Tve}^{(i)}$. Without loss of generality, we assume that $n_s \geq n_t$ for the Tversky similarity calculation below. Then, given a cross-network node pair (u, v) , we evaluate how many ACNs are shared between two sets $\mathcal{N}_{G_s, u}$ and $\mathcal{N}_{G_t, v}$, indicating one-hop neighbors of nodes $u \in \mathcal{V}_s$ and $v \in \mathcal{V}_t$, respectively, upon the one-to-one node mapping $\pi^{(i)}$. To this end, we characterize the Tversky similarity $\mathbf{S}_{Tve}^{(i)}(u, v)$ between two nodes $u \in \mathcal{V}_s$ and $v \in \mathcal{V}_t$ at the i -th iteration by means of the mapping $\pi^{(i)}$, which is formulated as:

$$\begin{aligned} & \mathbf{S}_{Tve}^{(i)}(u, v) \\ &= \frac{|X_u^{(i)} \cap Y_v^{(i)}|}{|X_u^{(i)} \cap Y_v^{(i)}| + \alpha |X_u^{(i)} - Y_v^{(i)}| + \beta |Y_v^{(i)} - X_u^{(i)}|}, \end{aligned} \quad (9)$$

where

$$\begin{aligned} \mathcal{T}_u^{(i)} &= \left\{ \pi^{(i)}(x) \mid x \in \left(\mathcal{N}_{G_s, u} \cap \tilde{\mathcal{V}}_s^{(i)} \right) \right\} \\ X_u^{(i)} &= \left(\mathcal{N}_{G_s, u} - \tilde{\mathcal{V}}_s^{(i)} \right) \cup \mathcal{T}_u^{(i)} \\ Y_v^{(i)} &= \mathcal{N}_{G_t, v}. \end{aligned} \quad (10)$$

Here, $\tilde{\mathcal{V}}_s^{(i)}$ is the set of *seed nodes* at the i -th iteration of gradual alignment in G_s , which is defined as the union of already aligned node pairs up to the i -th iteration and $\tilde{\mathcal{V}}_s^{(0)}$ (i.e., prior seed nodes in G_s); and $\alpha, \beta > 0$ are the parameters of the Tversky index. In our study, we set $0 < \alpha < 1$ and $\beta = 1$ under the condition $n_s \geq n_t$, where the appropriate value of α will be numerically found in Section 5.5.2. It is worth noting that the case of $\alpha = \beta = 1$ corresponds to the Tanimoto coefficient (also known as the Jaccard index) [12], which can be seen as a symmetric set similarity measure. In particular, we would like to address the importance of the parameter setting in our Tversky similarity.

Remark 1. *The parameter α in (9) plays a crucial role in balancing between $|X_u^{(i)} \cap Y_v^{(i)}|$ (i.e., the number of ACNs of node pair (u, v)) and $|X_u^{(i)} - Y_v^{(i)}|$ (i.e., the cardinality of the set difference of $X_u^{(i)}$ and $Y_v^{(i)}$). More specially, for $n_s \gg n_t$, a number of nodes in G_s remain unaligned even when the alignment process is completed; thus, the term $|X_u^{(i)} \cap Y_v^{(i)}|$ would be far smaller than $|X_u^{(i)} - Y_v^{(i)}|$.⁷ In this case, we are capable of more precisely calculating the similarity between node pairs of two networks that are severely imbalanced during the gradual alignment by adjusting the value of α accordingly. By setting $0 < \alpha < 1$, we can mitigate the impact of $|X_u^{(i)} - Y_v^{(i)}|$ so that $|X_u^{(i)} \cap Y_v^{(i)}|$ is relatively influential.*

Since the number of ACNs is expected to increase over iterations in gradual alignment, we are interested in investigating how fast the Tversky similarity $\mathbf{S}_{Tve}^{(i)}(u, v)$ grows with respect to the number of ACNs. To see the impact and benefits of the Tversky similarity in terms of its growth rate, we analytically show the effectiveness of the Tversky similarity with a proper parameter setting by establishing the following theorem.

Theorem 4.2. *Given a node pair (u, v) , suppose that $|Y_v^{(i)} - X_u^{(i)}| \geq |X_u^{(i)} \cap Y_v^{(i)}|$ for all gradual alignment steps. Then, under the condition $n_s \geq n_t$, the growth rate of our Tversky similarity $\mathbf{S}_{Tve}^{(i)}(u, v)$ using $0 < \alpha < 1$ and $\beta = 1$ with respect to $|X_u^{(i)} \cap Y_v^{(i)}|$ (i.e., the number of ACNs of node pair (u, v) at the i -th iteration) is always higher than that of the Jaccard index using $\alpha = \beta = 1$.*

Proof. Let $\mathbf{S}_{Jac}^{(i)}(u, v)$ denote the Jaccard index between two nodes $u \in \mathcal{V}_s$ and $v \in \mathcal{V}_t$ in the i -th iteration. For notational convenience, by denoting $a = |X_u^{(i)} - Y_v^{(i)}|$, $b = |Y_v^{(i)} - X_u^{(i)}|$, and $c = |X_u^{(i)} \cap Y_v^{(i)}|$ for $b \geq c \geq 0$, we have

$$\begin{aligned} \mathbf{S}_{Tve}^{(i)}(u, v) &= \frac{c}{\alpha a + b + c} = 1 - \frac{\alpha a + b}{\alpha a + b + c} \\ \mathbf{S}_{Jac}^{(i)}(u, v) &= \frac{c}{a + b + c} = 1 - \frac{a + b}{a + b + c}. \end{aligned} \quad (11)$$

⁷ We empirically validated that over 99% out of all node pairs meet this condition (i.e., $|X_u^{(i)} \cap Y_v^{(i)}| \ll |X_u^{(i)} - Y_v^{(i)}|$) in the gradual alignment process in three real-world datasets under consideration.

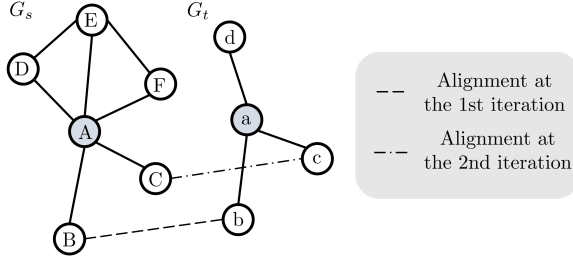


Fig. 4: An example illustrating gradual alignment of two networks G_s and G_t with $n_s = 6$ and $n_t = 4$.

Then, the difference between the growth rates of $\mathbf{S}_{Tve}^{(i)}(u, v)$ and $\mathbf{S}_{Jac}^{(i)}(u, v)$ with respect to c is given by

$$\begin{aligned} \frac{\partial \mathbf{S}_{Jac}^{(i)}(u, v)}{\partial c} - \frac{\partial \mathbf{S}_{Tve}^{(i)}(u, v)}{\partial c} &= \frac{w_1}{(w_1 + c)^2} - \frac{w_2}{(w_2 + c)^2} \\ &= \frac{(w_1 - w_2)(c^2 - w_1 w_2)}{(w_1 + c)^2 (w_2 + c)^2}, \end{aligned} \quad (12)$$

where $w_1 = a + b$ and $w_2 = \alpha a + b$. Here, due to the fact that $w_1 - w_2 = (1 - \alpha)a \geq 0$, $w_1 \geq c$, and $w_2 \geq c$, it follows that

$$\frac{\partial \mathbf{S}_{Tve}^{(i)}(u, v)}{\partial c} \geq \frac{\partial \mathbf{S}_{Jac}^{(i)}(u, v)}{\partial c}, \quad (13)$$

which completes the proof of this theorem. \square

By Theorem 4.2, using the parameter setting $0 < \alpha < 1$ and $\beta = 1$ in the Tversky similarity facilitates the increase of the similarity level during the gradual alignment, thus better capturing the topological consistency. In other words, we can make full use of the benefits of gradual alignment along with high growth rates of Tversky similarity with respect to $|X_u^{(i)} \cap Y_v^{(i)}|$ over iterations, which thereby results in improved alignment accuracy.

Example 1. We show how using the Tversky similarity $\mathbf{S}_{Tve}^{(i)}(u, v)$ is beneficial over the Jaccard index $\mathbf{S}_{Jac}^{(i)}(u, v)$ in terms of capturing the topological consistency of cross-network node pairs. As illustrated in Fig. 4, consider two networks G_s and G_t with $n_s = 6$ and $n_t = 4$, where there is a single matched pair (B,b) such that $\mathcal{T}_A^{(1)} = \{b\}$, $X_A^{(1)} = \{b, C, D, E, F\}$, $Y_a^{(1)} = \{b, c, d\}$, and $X_A^{(1)} \cap Y_a^{(1)} = \{b\}$. Suppose that $\alpha = \frac{1}{2}$ and $\beta = 1$. Then, we have $\mathbf{S}_{Tve}^{(1)}(A, a) = \frac{1}{5}$ and $\mathbf{S}_{Jac}^{(1)}(A, a) = \frac{1}{7}$. At the next gradual alignment step, we assume that (C,c) is newly aligned, which leads to $X_A^{(2)} = \{b, c, D, E, F\}$, $Y_a^{(2)} = \{b, c, d\}$, and $X_A^{(2)} \cap Y_a^{(2)} = \{b, c\}$. Then, it follows that $\mathbf{S}_{Tve}^{(2)}(A, a) = \frac{4}{9}$ and $\mathbf{S}_{Jac}^{(2)}(A, a) = \frac{2}{7}$. Since the growth rate of the Tversky similarity and the Jaccard index with respect to the number of ACNs is given by $\frac{11}{45}$ and $\frac{1}{7}$, respectively, using the Tversky similarity is beneficial in terms of better capturing the structural consistency across different networks, which finally leads to performance improvement.

After calculating our dual-perception similarity matrix $\mathbf{S}^{(i)}$ in (2) based on two similarity matrices \mathbf{S}_{emb} and $\mathbf{S}_{Tve}^{(i)}$, we gradually match N node pairs for each iteration until all M node pairs are found. Let us explain how to choose N node pairs per iteration as follows. At the first iteration,

we find the most confident pair (i.e., an element with the highest value) out of $n_s n_t$ elements in $\mathbf{S}^{(1)}$ and then find the second most confident pair among $(n_s - 1)(n_t - 1)$ elements after deleting all elements related to the most confident pair. We repeatedly perform the above steps until N node pairs are matched for the first iteration. Updating the node mapping $\pi^{(i)}$, we recalculate $\mathbf{S}_{Tve}^{(i+1)}$ to discover N node pairs at the next iteration. This process is repeated at each iteration. We refer to lines 18–22 in Algorithm 1 for calculation of $\mathbf{S}^{(i+1)}$ upon the updated one-to-one node mapping $\pi^{(i+1)}$.

4.2 Complexity Analysis

In this subsection, we analyze the computational complexity of Grad-Align. When an untrained GNN model is used, the complexity of the multi-layer embedding similarity can be analyzed below. In the feed-forward process, the computational complexity of message passing over all GNN layers is given by $\mathcal{O}(L \max\{|\mathcal{E}_s|, |\mathcal{E}_t|\})$ [30], where L is the number of GNN layers, and \mathcal{E}_s and \mathcal{E}_t are the numbers of edges in G_s and G_t , respectively. While the element-wise calculation of the similarity matrix \mathbf{S}_{emb} in (1) is repeated $n_s n_t$ times [19], this process is computable in constant time when parallelization is applied. Now, we are ready to show the following theorem, which states a comprehensive analysis of the total complexity.

Theorem 4.3. *The computational complexity of the proposed Grad-Align method is given by $\mathcal{O}(\max\{|\mathcal{E}_s|, |\mathcal{E}_t|\})$.*

Proof. For a given node pair (u, v) , we focus on analyzing the computational complexity of the Tversky similarity calculation. Since we take into account one-hop neighbors of each node in handling each term in (9), the complexity of calculating $|X_u^{(i)} - Y_v^{(i)}|$, $|Y_v^{(i)} - X_u^{(i)}|$, and $|X_u^{(i)} \cap Y_v^{(i)}|$ is given by $\mathcal{O}(|X_u^{(i)}|)$, $\mathcal{O}(|Y_v^{(i)}|)$, and $\mathcal{O}(|X_u^{(i)}| |Y_v^{(i)}|)$, respectively, for the worst case, which are bounded by the maximum node degree in G_s and G_t and thus are regarded as a constant. As in the calculation of \mathbf{S}_{emb} , the Tversky similarity matrix $\mathbf{S}_{Tve}^{(i)}$ is computable in constant time due to the independent element-wise calculation via parallel processing. From the fact that the number of iterations for gradual alignment is finite and the computation of \mathbf{S}_{emb} is a bottleneck, the total complexity of our Grad-Align method is finally bounded by $\mathcal{O}(\max\{|\mathcal{E}_s|, |\mathcal{E}_t|\})$. This completes the proof of this theorem. \square

From Theorem 4.3, one can see that the computational complexity of Grad-Align scales linearly with the maximum number of edges over two networks. This also implies that the computational complexity of Grad-Align scales no larger than that of the embedding similarity calculation using the underlying GNN model.

4.3 Grad-Align-EA Method

In this subsection, we introduce Grad-Align-EA, namely Grad-Align with edge augmentation, to further improve the performance of Grad-Align by incorporating an edge augmentation module into the Grad-Align method, which is inspired by CENALP [19] that jointly performs NA and link prediction. However, different from the link prediction

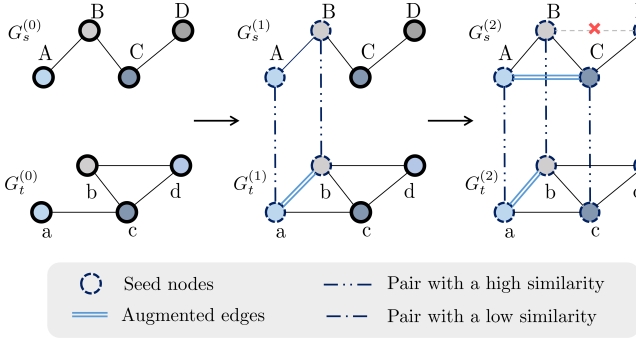


Fig. 5: An example illustrating edge augmentation over iterations. Here, the edge between nodes (a, b) in G_t is augmented at the first step, and the edge between nodes (A, C) is augmented at the second step.

in CENALP that requires the high computational cost, our edge augmentation only creates edges that are *highly confident* without any training and test phases. The edge augmentation makes both networks G_s and G_t evolve in such a way that their structural consistencies across the networks are getting high over iterations in the gradual alignment process. To express the evolution of each network, we rewrite source and target networks as $G_s^{(i)} = (\mathcal{V}_s, \mathcal{E}_s^{(i)}, \mathcal{X}_s)$, $G_t^{(i)} = (\mathcal{V}_t, \mathcal{E}_t^{(i)}, \mathcal{X}_t)$, respectively, where $\mathcal{E}_s^{(i)}$ and $\mathcal{E}_t^{(i)}$ are the sets of edges in $G_s^{(i)}$ and $G_t^{(i)}$, respectively. The overall procedure of our edge augmentation is summarized in Algorithm 2.⁸ Let $\tilde{\mathcal{E}}_s$ ($\tilde{\mathcal{E}}_t$) denote the set of *potentially confident edges* that are not in the set $\mathcal{E}_s^{(i)}$ ($\mathcal{E}_t^{(i)}$) while their counterpart edges upon the node mapping $\pi^{(i)}$ are in $\mathcal{E}_t^{(i)}$ ($\mathcal{E}_s^{(i)}$). If the aligned node pair does not match the ground truth, then the augmented edge will be treated as noise in the next alignment step. To remedy this problem, our edge augmentation module creates edges among potentially confident ones only when they are strongly confident. More specifically, we augment edges only when the dual-perception similarity $\mathbf{S}^{(i)}(u, v)$ of node pair (u, v) is greater than a certain threshold $\tau > 0$ (refer to lines 3 and 9 in Algorithm 2), where τ will be set appropriately in Section 5.5.5. Fig. 5 illustrate an example of edge augmentation over iterations in our Grad-Align-EA. In the first step, the potentially confident edge between nodes (a, b) in G_t is augmented. In the second step, the edge between nodes (A, C) is augmented but another potentially confident edge between nodes (B, D) is not augmented because $\mathbf{S}^{(i)}(D, d)$ is not sufficiently high.

Since the structure of each network evolves over iterations via the edge augmentation module, we need to newly update the hidden representations of each network by re-training model parameters θ of GNN and then recalculate the multi-layer embedding similarity matrix. In this context, the dual-perception similarity matrix in (2) is rewritten as

$$\mathbf{S}^{(i)} = \mathbf{S}_{emb}^{(i)} \odot \mathbf{S}_{Tve}^{(i)}, \quad (14)$$

⁸The source code for Grad-Align-EA is available online (<https://github.com/jindeok/Grad-Align-full/tree/main/Grad-Align-EA>).

Algorithm 2 Edge augmentation

Input: $G_s^{(i)} = (\mathcal{V}_s, \mathcal{E}_s^{(i)}, \mathcal{X}_s)$, $G_t^{(i)} = (\mathcal{V}_t, \mathcal{E}_t^{(i)}, \mathcal{X}_t)$, $\pi^{(i)}$, $\mathbf{S}^{(i)}$, $\tilde{\mathcal{E}}_s, \tilde{\mathcal{E}}_t, \tau$

Output: $G_s^{(i+1)}, G_t^{(i+1)}$

- 1: /* Edge augmentation for $G_s^{(i)}$ */
- 2: **for** $(u_1, u_2) \in \tilde{\mathcal{E}}_s$ **do**
- 3: **if** $\mathbf{S}^{(i)}(u, \pi^{(i)}(u)) > \tau$ and $\mathbf{S}^{(i)}(v, \pi^{(i)}(v)) > \tau$ **then**
- 4: $\mathcal{E}_s^{(i+1)} = \mathcal{E}_s^{(i)} \cup \{(u, v)\}$
- 5: **end if**
- 6: **end for**
- 7: /* Edge augmentation for $G_t^{(i)}$ */
- 8: **for** $(v_1, v_2) \in \tilde{\mathcal{E}}_t$ **do**
- 9: **if** $\mathbf{S}^{(i)}(\pi^{-1(i)}(u'), u') > \tau$ and $\mathbf{S}^{(i)}(\pi^{-1(i)}(v'), v') > \tau$ **then**
- 10: $\mathcal{E}_t^{(i+1)} = \mathcal{E}_t^{(i)} \cup \{(u', v')\}$
- 11: **end if**
- 12: **end for**
- 13: **return** $G_s^{(i+1)} = (\mathcal{V}_s, \mathcal{E}_s^{(i+1)}, \mathcal{X}_s)$,
 $G_t^{(i+1)} = (\mathcal{V}_t, \mathcal{E}_t^{(i+1)}, \mathcal{X}_t)$

Datasets		# of nodes	# of edges	# of attributes	# of ground truth node pairs
Facebook	G_s	1,043	4,734	0	1,043
Twitter	G_t	1,043	4,860	0	
Douban Online	G_s	3,906	8,164	538	1,118
Douban Offline	G_t	1,118	1,511	538	
Allmovie	G_s	6,011	124,709	14	5,176
IMDb	G_t	5,713	119,073	14	
Facebook (Its noisy version)	G_s	1,256	4,260	0	1,043
	G_t	1,256	4,256	0	
Econ (Its noisy version)	G_s	1,258	6,857	20	1,258
	G_t	1,258	6,860	20	
DBLP (Its noisy version)	G_s	2,151	5,676	20	2,158
	G_t	2,151	5,672	20	
Foursquare (Its noisy version)	G_s	17,355	132,208	0	17,355
	G_t	17,355	131,018	0	

TABLE 2: Statistics of the seven datasets used in our experiments.

where $\mathbf{S}_{emb}^{(i)}$ represents the multi-layer embedding similarity matrix at the i -th iteration when Grad-Align-EA is used.

5 EXPERIMENTAL EVALUATION

In this section, we first describe datasets used in the evaluation. We also present five state-of-the-art NA methods for comparison. After presenting performance metrics and our experimental settings, we comprehensively evaluate the performance of our Grad-Align method and five benchmark methods.

5.1 Datasets

We conduct experiments on several real-world and synthetic datasets across various domains, which are widely adopted for evaluating the performance of NA. The main statistics of each dataset, including the number of nodes, the number of edges, the number of attributes, and the number of node pairs, are summarized in Table 2. In the following, we explain important characteristics of the datasets briefly.

5.1.1 Real-World Datasets

We use three real-world datasets, each of which consists of two networks (i.e., source and target networks).

Facebook vs. Twitter (Fb-Tw). The Fb-Tw dataset is composed of two real-world social networks collected and published by [31]. User accounts and friendships of accounts are treated as nodes and edges, respectively.

Douban Online vs. Douban Offline (Douban). The Douban dataset is a Chinese social network collected and published by [11]. User accounts and their friendships are treated as nodes and edges, respectively.

Allmovie vs. IMDb (Am-ID). The Allmovie network is constructed from Rotten Tomatoes (an American review-aggregation website), where films are treated as nodes and two films have an edge connecting them if they have at least one common actor.⁹ The IMDb network is constructed from IMDb (an online database of information on movies, TV, and celebrities).¹⁰ Its nodes and edges are created similarly as in Allmovie.

5.1.2 Synthetic Datasets

In addition to the above three real-world datasets, we synthesize network data to comprehensively evaluate noisy conditions on the network structure and node attributes similarly as in [2], [19]. From the original network, we generate its noisy version by randomly removing a certain number of edges and replacing a portion of node attributes with zeros, while preserving the number of ground truth cross-network node pairs. We use four synthetic datasets, consisting of two non-attributed networks and two attributed networks, as follows.

Facebook. The Facebook network is originated from the source network of the Fb-Tw dataset in Section 5.1.1.

Econ. The Econ network is an economic model of Victoria state, Australia during the banking crisis in 1880 [2], [32]. The nodes and edges represent the organizations located in the state and the contractual relationships between them, respectively.

DBLP. The DBLP dataset is a co-authorship network collected and published by [33]. Authors and their academic interactions are treated as nodes and edges, respectively. An attribute vector represents the number of publications in computer science conferences [19].

Foursquare. The Foursquare dataset is a location-based online social network and is originally collected by [13]. The nodes and edges represent the users and the follower/followee relationships between them, respectively.

5.2 State-of-the-Art Methods

In this subsection, we present five state-of-the-art NA methods for comparison.

GAlign [2]. This is an unsupervised NA method based on a multi-order GCN model using local and global structural information, where prior seed nodes are not available.

CENALP [19]. This method jointly performs NA and link prediction tasks to improve the alignment accuracy. A cross-network embedding strategy is employed based on a variant of DeepWalk [34].

⁹. <https://www.kaggle.com/ayushkalla1/rotten-tomatoes-movie-database>.

¹⁰. <https://www.kaggle.com/jyoti1706/IMDbmoviesdataset>.

FINAL [1]. This method aligns attributed networks based on the alignment consistency principle. Specifically, FINAL utilizes three consistency conditions including the topology consistency, node attribute consistency, and edge attribute consistency.

PALE [7]. This is a supervised NA model that employs network embedding with awareness of prior seed nodes and learns a cross-network mapping via an MLP architecture for NA.

DeepLink [3]. This model encodes nodes into vector representations to capture local and global network structures through deep neural networks in a semi-supervised learning manner.

5.3 Performance Metrics

To assess the performance of our proposed Grad-Align method and the five state-of-the-art methods, as the most popular metric, we adopt the *alignment accuracy* [1], [19], denoted as *Acc*, which quantifies the proportion of correct node correspondences out of the total M correspondences. We also adopt *Precision@q* (also known as *Success@q*) as another performance metric as in [1], [2], [3], which indicates whether there is the true positive matching identity in top- q candidates and is expressed as

$$Precision@q = \frac{\sum_{v_s^* \in \mathcal{V}_s} \mathbb{1}_{v_t^* \in \mathcal{S}^q(v_s^*)}}{M}, \quad (15)$$

where (v_s^*, v_t^*) is each node pair in the ground truth; $\mathcal{S}^q(v_s^*)$ indicates the set of indices of top- q elements in the v_s^* -th row of the dual-perception similarity matrix $\mathbf{S}^{(\lceil \frac{M}{N} \rceil + 1)}$ in (2); and $\mathbb{1}_{\mathcal{S}^q(v_s^*)}$ is the indicator function. For node v_s^* , if the similarity $\mathbf{S}^{(\lceil \frac{M}{N} \rceil + 1)}(v_s^*, v_t^*)$ is ranked within the q -th highest values in the row $\mathbf{S}^{(\lceil \frac{M}{N} \rceil + 1)}(v_s^*, :)$ of the similarity matrix $\mathbf{S}^{(\lceil \frac{M}{N} \rceil + 1)}$, then the alignment output for v_s^* is recorded as a successful case. Note that the higher the value of each of the two metrics, the better the performance.

5.4 Experimental Setup

We describe experimental settings of neural networks (i.e., the GNN model) in our Grad-Align method. The GNN model is implemented by PyTorch Geometric [35], which is a geometric deep learning extension library in PyTorch. We set the dimension of each GNN hidden layer as 150. We train our GNN model using Adam optimizer [36] with a learning rate of 0.005. Since Fb-Tw, Facebook (and its noisy version), and Foursquare (and its noisy version) datasets do not contain node attributes, we use all-ones vectors $\mathbf{1} \in \mathbb{R}^{1 \times n_s}$ and $\mathbf{1} \in \mathbb{R}^{1 \times n_t}$ as the input node attribute vectors for the GNN model on the datasets. We use the following key hyperparameters in Grad-Align.

- The number of GNN layers (k);
- Coefficients of the Tversky index in (9) (α and β);
- The number of iterations for gradual matching ($iter = \lceil \frac{M}{N} \rceil + 1$);
- The proportion of prior seed node pairs out of M ground truth node pairs (t).

In our experiments, the above hyperparameters are set to the pivot values $k = 2$, $\alpha = \frac{n_s}{n_t}$, $\beta = 1$, $iter = 15$, and $t = 0.1$ unless otherwise stated.

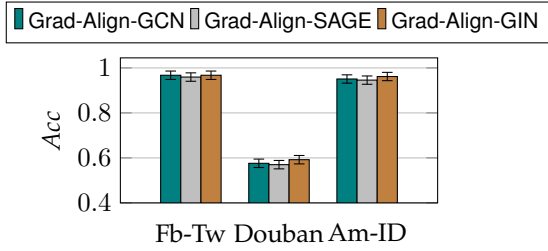


Fig. 6: Alignment accuracy according to different GNN models in our Grad-Align method on the three real-world datasets.

Next, as a default experimental setting for all the methods, 10% of ground truth node correspondences are randomly selected and used as the training set over all the datasets as in [2]. For each synthetic dataset in Section 5.1.2, to generate its noisy version, we randomly remove 10% of edges and replace 10% of node attributes with zeros unless otherwise specified. We conduct each experiment over 10 different random seeds to evaluate the average performance. All experiments are carried out with Intel (R) 12-Core (TM) i7-9700K CPUs @ 3.60 GHz and 32GB RAM.

5.5 Experimental Results

In this subsection, our extensive empirical study is designed to answer the following six key research questions.

- Q1. How do underlying GNN models affect the performance of the Grad-Align method?
- Q2. How do model hyperparameters affect the performance of the Grad-Align method?
- Q3. How much does the Grad-Align method improve the NA performance over state-of-the-art NA methods?
- Q4. How robust is our Grad-Align method to more difficult settings with high structural/attribute noise levels?
- Q5. How much does each component in the Grad-Align method contribute to the performance?
- Q6. How expensive is the computational complexity of Grad-Align in comparison with state-of-the-art NA methods?

To answer the research questions stated above, we comprehensively carry out experiments in the following.

5.5.1 Comparative Study Among GNN Models (Q1)

In Fig. 6, we show the performance on *Acc* of various GNN models in Grad-Align using three real-world datasets. Since our method is *GNN-model-agnostic*, any existing models can be adopted; however, in our experiments, we adopt the following three milestone GNN models from the literature, namely GCN [20] (Grad-Align-GCN), GraphSAGE [21] (Grad-Align-SAGE), and GIN [22] (Grad-Align-GIN).¹¹ Here, we use the sum aggregator as a default AGGREGATE function in (3).

11. For the GIN model, we use a two-layer MLP architecture and the ReLU activation function [37] according to the original implementation in [22].

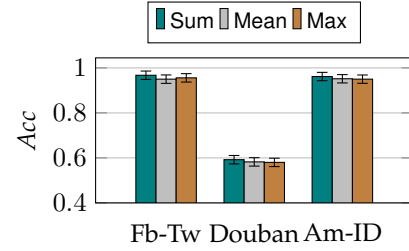


Fig. 7: Alignment accuracy according to different aggregators in our Grad-Align method on the three real-world datasets.

From Fig. 6, it is seen that Grad-Align-GIN consistently outperforms other models regardless of the datasets although the gains over other models are not significant. It is worth noting that GIN was proposed to generalize the Weisfeiler-Lehman (WL) graph isomorphism test to achieve its maximum discriminative power among GNNs [22]. Due to the fact that the higher the expressiveness of the node representation, the more probable it is to find the correct node correspondence without any ambiguity, the GIN model-aided approach (i.e., Grad-Align-GIN) achieves the best performance with a more expressive power.

In Fig. 7, we show how *Acc* performance behaves according to several AGGREGATE functions in (3), including the sum, mean, and max aggregators, when Grad-Align-GIN is used for the three real-world datasets. It is observed that the sum aggregator has the most expressive power among three AGGREGATE functions while achieving the highest *Acc*. This finding is consistent with the statements in [22].

From the intriguing observations stated above, we use Grad-Align-GIN with sum aggregation in our subsequent experiments.

5.5.2 Effect of Hyperparameters (Q2)

In Fig. 8, we investigate the impact of four key hyperparameters, including k , α , $iter$, and t addressed in Section 5.4, on the performance of Grad-Align in terms of the *Acc* score using three real-world datasets. When a hyperparameter varies so that its effect is clearly revealed, other parameters are set to the pivot values in Section 5.4. Our findings are as follows.

- **The effect of k :** From Fig. 8a, setting $k = 2$ consistently leads to the best performance for all the datasets. If $k < 2$, then the proximity information is limited to the direct neighbors, which can be vulnerable to structural and attribute inconsistencies of nodes. If $k > 2$, then our Grad-Align method may experience the oversmoothing problem for GNNs [38].
- **The effect of α :** From Theorem 4.2, we recall that using the Tversky similarity is beneficial in conducting the NA task compared to the case of the Jaccard similarity (i.e., $\alpha = \beta = 1$). From Fig. 8b, we show that setting α near $\frac{n_t}{n_s}$ achieves the best performance for all the datasets, where $\frac{n_t}{n_s}$ corresponds to 1, 0.29, and 0.95 for the Fb-Tw, Douban, and Am-ID datasets, respectively. This empirical finding is vital in the

Dataset	Metric	Grad-Align	GAlign	CENALP	FINAL	PALE	DeepLink
Fb-Tw	<i>Acc</i>	<u>0.9674</u>	0.0513	0.8566	0.8571	0.7963	0.2520
	<i>Precision@1</i>	<u>0.9674</u>	0.0306	0.5781	0.6007	0.5295	0.1151
	<i>Precision@5</i>	<u>0.9856</u>	0.0422	0.7220	0.7864	0.7854	0.2927
	<i>Precision@10</i>	<u>0.9904</u>	0.0612	0.7661	0.7773	0.8803	0.3350
Douban	<i>Acc</i>	<u>0.5921</u>	0.2568	0.1350	0.3373	0.1852	0.1011
	<i>Precision@1</i>	<u>0.6682</u>	0.3686	0.1571	0.3479	0.1377	0.0921
	<i>Precision@5</i>	<u>0.8551</u>	0.5233	0.2584	0.5134	0.3283	0.2290
	<i>Precision@10</i>	<u>0.8980</u>	0.6324	0.3618	0.6764	0.4338	0.2907
Am-ID	<i>Acc</i>	<u>0.9568</u>	0.7364	0.5212	0.7725	0.7397	0.2780
	<i>Precision@1</i>	<u>0.9601</u>	0.7251	0.4566	0.6524	0.5793	0.1361
	<i>Precision@5</i>	<u>0.9744</u>	0.8101	0.6657	0.8594	0.8242	0.3327
	<i>Precision@10</i>	<u>0.9783</u>	0.8749	0.8127	0.8945	0.8519	0.4650
Facebook & its noisy version	<i>Acc</i>	<u>0.9396</u>	0.0413	0.8174	0.6072	0.6079	0.2780
	<i>Precision@1</i>	<u>0.9415</u>	0.0406	0.8174	0.5004	0.5279	0.1361
	<i>Precision@5</i>	<u>0.9962</u>	0.0622	0.8523	0.5509	0.6040	0.3327
	<i>Precision@10</i>	<u>0.9987</u>	0.0899	0.9175	0.8954	0.7162	0.4650
Econ & its noisy version	<i>Acc</i>	<u>0.9841</u>	0.8953	0.5509	0.4948	0.5819	0.2583
	<i>Precision@1</i>	<u>0.9873</u>	0.8647	0.4247	0.4434	0.3060	0.1161
	<i>Precision@5</i>	<u>0.9960</u>	0.9100	0.5658	0.5642	0.6041	0.2671
	<i>Precision@10</i>	<u>0.9968</u>	0.9346	0.7112	0.5944	0.6836	0.3506
DBLP & its noisy version	<i>Acc</i>	<u>0.9350</u>	0.9126	0.6458	0.7646	0.3436	0.1413
	<i>Precision@1</i>	<u>0.9292</u>	0.8914	0.5992	0.7785	0.1437	0.0656
	<i>Precision@5</i>	<u>0.9778</u>	0.9340	0.6528	0.7954	0.3622	0.1957
	<i>Precision@10</i>	<u>0.9990</u>	0.9623	0.7775	0.8164	0.4826	0.2748
Foursquare & its noisy version	<i>Acc</i>	<u>0.8998</u>	0.0241	0.8128	0.5214	0.3872	0.1374
	<i>Precision@1</i>	<u>0.8992</u>	0.0214	0.8112	0.5074	0.3778	0.1352
	<i>Precision@5</i>	<u>0.9128</u>	0.0287	0.8424	0.5876	0.3958	0.1627
	<i>Precision@10</i>	<u>0.9344</u>	0.0397	0.8875	0.6124	0.4124	0.1871

TABLE 3: Performance comparison among Grad-Align and state-of-the-art NA methods in terms of the *Acc* and *Precision@q*. Here, the best method for each case is highlighted using underlines.

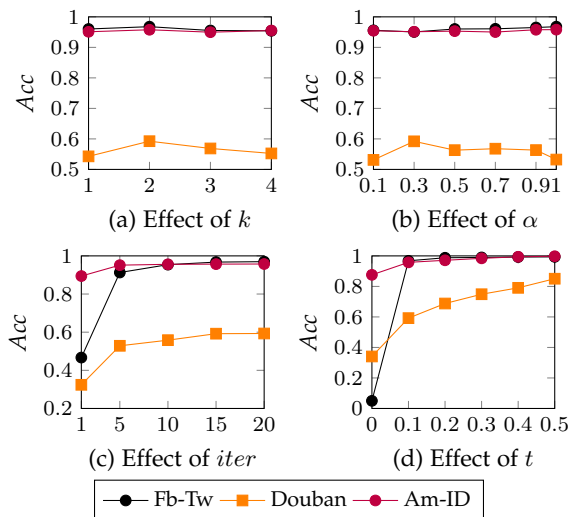


Fig. 8: Alignment accuracy according to different values of hyperparameters in our Grad-Align method on the three real-world datasets.

design perspective. Specifically, by setting $\alpha \simeq \frac{n_t}{n_s}$ according to the ratio of the number of nodes in two unbalanced networks, we are capable of balancing between two terms in (9), $|X_u^{(i)} - Y_v^{(i)}|$ and $|Y_v^{(i)} - X_u^{(i)}|$, which thus enhances the degree of topological consistency across the two networks and then improves the alignment accuracy. This demon-

strates the effectiveness of our Tversky similarity with proper parameter settings.

- **The effect of *iter*:** In Fig. 8c, the performance is improved with increasing *iter* regardless of the datasets, which verifies the power of gradual alignment. It is also worthwhile to note that using only a small number of iterations for some datasets (e.g., *iter* = 5 for Am-ID) is sufficient to achieve a significant gain over the case of finding all node correspondences at once (i.e., *iter* = 1).
- **The effect of *t*:** As shown in Fig. 8d, one can see that dramatic gains are possible by exploiting prior seed nodes. For the non-attributed network such as Fb-Tw, the case of *t* = 0 performs quite poorly. This is because it is difficult to precisely compute the multi-layer embedding similarity S_{emb} when node attributes are unavailable; thus, the Tversky similarity calculation with prior seed nodes plays a crucial role in correctly finding node correspondences for such non-attributed networks. On the other hand, for attributed networks such as Douban and Am-ID, satisfactory performance is observed even when *t* = 0.

5.5.3 Comparison with State-of-the-Art Approaches (Q3)

The performance comparison between our Grad-Align method and five state-of-the-art NA methods, including GAlign [2], CENALP [19], FINAL [1], PALE [7], and DeepLink [3], is comprehensively presented in Table 3 with respect to *Acc* and *Precision@q* using three real-world and

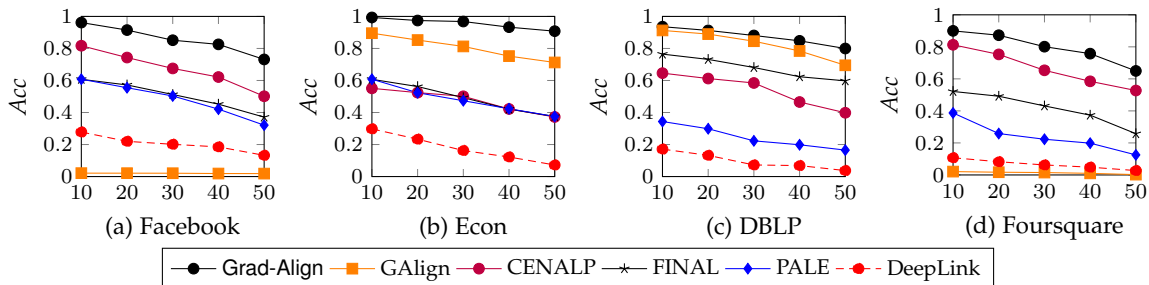


Fig. 9: Alignment accuracy according to different levels of the structural noise (%) on four synthetic datasets.

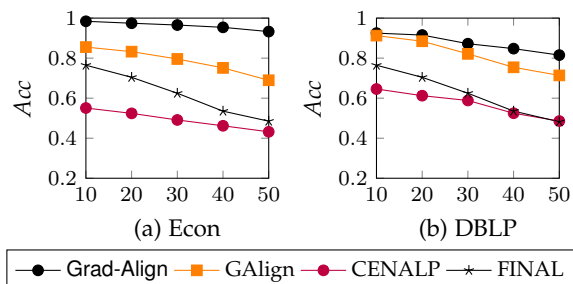


Fig. 10: Alignment accuracy according to different levels of the attribute noise (%) on two synthetic datasets.

four synthetic datasets. We note that the hyperparameters in all the aforementioned state-of-the-art methods are tuned differently according to each individual dataset so as to provide the best performance. In Table 3, the value with an underline indicates the best performer for each case. We would like to make the following insightful observations:

- Our Grad-Align method consistently and significantly outperforms all the state-of-the-art methods regardless of the datasets and the performance metrics.
- The second-best performer depends on the datasets, which implies that one does not dominate others among the five state-of-the-art NA methods.
- The performance gap between our Grad-Align method (X) and the second-best performer (Y) is the largest when the Douban dataset is used; the maximum improvement rate of 75.54% is achieved in terms of Acc , where the improvement rate (%) is given by $\frac{X-Y}{Y} \times 100$.
- The Douban dataset is relatively challenging since it exhibits not only quite different scales between two networks G_s and G_t but also the inconsistent network topological structure between G_s and G_t [1], [19]. In the dataset, FINAL and GAlign, corresponding to the second and third best performers, respectively, perform satisfactorily by taking advantage of node attribute information; however, other NA methods such as CENALP, PALE, and DeepLink that depend heavily on the topological structure do not perform well.
- For the non-attributed networks such as Fb-Tw, Facebook (and its noisy version), and Foursquare (and its noisy version), Grad-Align is far superior to state-of-the-art methods. In such datasets, GAlign built upon the GCN model performs the worst. This implies that

designing a NA method based solely on GNN models would not guarantee satisfactory performance.

- Let us discuss the performance regarding four synthetic datasets. As addressed before, GAlign is quite inferior to other methods on Facebook (not having node attributes), but becomes the second-best performer on Econ and DBLP (having node attributes). In contrast, CENALP and PALE reveal convincing results on Facebook but weakly perform on Econ and DBLP. This implies that state-of-the-art methods are highly dependent on either the topological consistency or the attribute consistency. However, our method is shown to be robust to both structural and attribute noises by virtue of the dual-perception similarity measures.

5.5.4 Robustness to Network Noises (Q4)

We now compare our Grad-Align method to the five state-of-the-art NA methods in more difficult settings that often occur in real environments: 1) the case in which a large portion of edges in two given networks G_s and G_t are removed and 2) the case in which a large portion of node attributes in G_s and G_t are missing and replaced with zeros. The performance on Acc is presented according to different structural and attribute noise levels in Figs. 9 and 10, respectively, using synthetic datasets.

- In Fig. 9, we show how Acc behaves when we randomly remove $\{10, \dots, 50\}\%$ of existing edges in each dataset. Our findings demonstrate that, while the performance tends to degrade with an increasing portion of missing edges for all the methods, our Grad-Align consistently achieves superior performance compared to state-of-the-art methods. It is also seen that Grad-Align tends to be quite robust to such structural noises especially for datasets

Method	Metric	Fb-Tw	Douban	Am-ID
Grad-Align	<i>Acc</i>	0.96	0.59	0.96
	<i>Precision@1</i>	0.96	0.67	0.96
	<i>Precision@5</i>	0.98	0.86	<u>0.97</u>
	<i>Precision@10</i>	<u>0.99</u>	0.90	<u>0.98</u>
Grad-Align-1	<i>Acc</i>	0.47	0.32	0.85
	<i>Precision@1</i>	0.47	0.42	0.87
	<i>Precision@5</i>	0.65	0.55	0.91
	<i>Precision@10</i>	0.77	0.71	0.94
Grad-Align-2	<i>Acc</i>	0.95	0.28	0.85
	<i>Precision@1</i>	0.95	0.38	0.86
	<i>Precision@5</i>	0.97	0.45	0.90
	<i>Precision@10</i>	0.98	0.55	0.95
Grad-Align-3	<i>Acc</i>	0.05	0.31	0.31
	<i>Precision@1</i>	0.07	0.41	0.37
	<i>Precision@5</i>	0.11	0.57	0.49
	<i>Precision@10</i>	0.17	0.68	0.58
Grad-Align-EA	<i>Acc</i>	<u>0.97</u>	<u>0.60</u>	<u>0.97</u>
	<i>Precision@1</i>	<u>0.97</u>	<u>0.68</u>	<u>0.97</u>
	<i>Precision@5</i>	<u>0.99</u>	<u>0.87</u>	<u>0.97</u>
	<i>Precision@10</i>	<u>0.99</u>	<u>0.91</u>	<u>0.98</u>

TABLE 4: Performance comparison among Grad-Align and its variants in terms of the *Acc* and *Precision@q* on the three real-world datasets. Here, the best case is highlighted using underlines.

having node attributes (i.e., Econ and DBLP). Moreover, since PALE and DeepLink depend solely on the structural consistency of nodes, the performance degradation is significant.

- In Fig. 10, we show how the performance varies when we randomly replace $\{10, \dots, 50\}$ % of node attributes in each dataset. Due to the fact that node attributes are unavailable on Facebook and Foursquare, the performance is presented using the Econ and DBLP datasets. It is verified that Grad-Align tends to be quite robust to node attribute noises.

It is worth noting that Grad-Align reveals strong robustness to the network noises especially for attributed networks. By virtue of the dual-perception similarity, our method is capable of bringing the synergy effect through reinforcing consistencies of nodes. In other words, when the structural noise increases, the embedding similarity plays an important role in guaranteeing high performance, while the Tversky similarity contributes more to the reliable performance as the attribute noise increases.

5.5.5 Impacts of Components in Grad-Align (Ablation Studies) (Q5)

In order to discover what role each component plays in the success of the proposed Grad-Align method, we conduct an ablation study by removing each module in our method. Additionally, we empirically show the gain of the edge augmentation module in Grad-Align.

- Grad-Align: This corresponds to the original Grad-Align method without removing any components.
- Grad-Align-1: The module of gradual alignment is removed. In other words, all node pairs are found at once using the dual-perception similarity $S^{(1)}$ (i.e., $iter = 1$).
- Grad-Align-2: The module of embedding similarity calculation is removed. That is, Grad-Align is performed only using $S_{Tve}^{(i)}$.

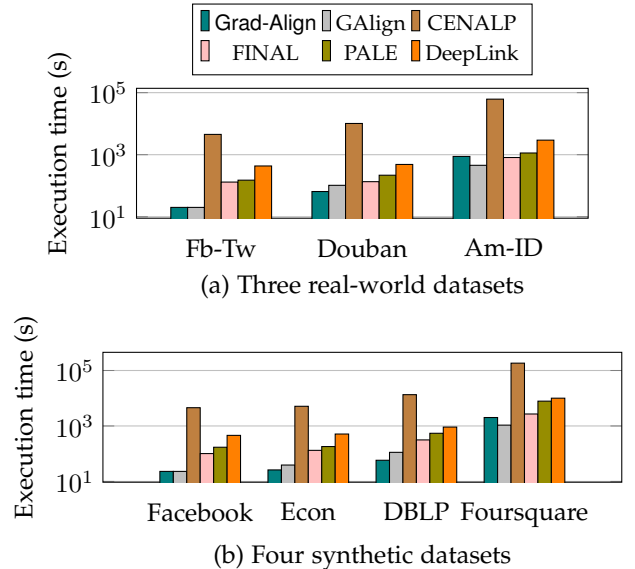


Fig. 11: The runtime complexity of Grad-Align and five state-of-the-art methods.

- Grad-Align-3: The module of Tversky similarity calculation is removed. That is, Grad-Align is performed only using S_{emb} .
- Grad-Align-EA: The edge augmentation module is added to our original Grad-Align method. The threshold τ is set to 0.7 for the three real-world datasets.

The performance comparison among the original Grad-Align and its variants, including three methods with each component removal and Grad-Align-EA, is presented in Table 4 with respect to *Acc* and *Precision@q* using three real-world datasets. In comparison with three methods with each component removal (i.e., ablation studies), one can see that the original Grad-Align method always exhibits potential gains over other variants, which demonstrate that each module plays a critical role together in discovering node correspondences. More interestingly, we observe that the performance gap between Grad-Align and Grad-Align-3 tends to be much higher than Grad-Align and other variants especially for the Fb-Tw dataset in which node attributes are not available. This finding indicates that the Tversky similarity calculation is indeed very crucial while the other modules further boost the performance as a supplementary role. Furthermore, in comparison with Grad-Align-EA, it is observed that the performance is enhanced compared to the original Grad-Align method since the edge augmentation module reinforces the structural consistency of given networks over iterations. However, such a gain is possible at the cost of extra computational complexities.

5.5.6 Computational Complexity (Q6)

To empirically validate the average runtime complexity of our Grad-Align method, we conduct experiments using the three real-world datasets as well as the four synthetic datasets whose number of nodes is sufficiently large (see Table 2). Fig. 11 illustrates the execution time (in seconds) of Grad-Align and five state-of-the-art methods on the three real-world datasets and the four synthetic datasets. It is seen

that CENALP has the highest runtime for all the datasets. On the other hand, the computational complexity of Grad-Align is competitive to that of light-weight models such as GAlign and FINAL. Besides, from Fig. 8c, due to the fact that reliable performance is still guaranteed even with small *iter* for the Am-ID dataset having the largest graph size, we can greatly reduce the runtime of Grad-Align by setting *iter* sufficiently small (e.g., *iter* = 5) while maintaining the satisfactory performance.

6 CONCLUDING REMARKS

In this paper, we explored an open yet important problem of how much gradual alignment in the NA task is beneficial over the discovery of all node pairs at once. To tackle this challenge, we introduced Grad-Align, a novel NA method that gradually aligns only a part of node pairs iteratively until all node pairs are found across two different networks by making full use of the information of already aligned node pairs having strong consistency in discovering weakly consistent node pairs. To realize our method, we proposed the dual-perception similarity consisting of the embedding similarity and the Tversky similarity. Specifically, we presented an approach to 1) calculating the similarity of multi-layer embeddings based on GNNs using the weight-sharing technique and the layer-wise reconstruction loss, 2) calculating the Tversky similarity to the network imbalance problem that often occurs in practice, and 3) iteratively updating our dual-perception similarity for gradual matching. Additionally, to boost the performance of the original Grad-Align, we developed Grad-Align-EA integrating an edge augmentation module into Grad-Align, which helps reinforce the structural consistency across different networks. Using various real-world and synthetic datasets, we demonstrated that our Grad-Align method remarkably outperforms all state-of-the-art NA methods in terms of the *Acc* and *Precision@q* while showing significant gains over the second-best performer by up to 75.54%. We also empirically validated the robustness of Grad-Align to both structural and attribute noises by virtue of our judiciously devised dual-perception similarity. Furthermore, not only the effect of key hyperparameters including α but also the impacts of each module in Grad-Align were comprehensively investigated.

Potential avenues of our future research include the design of an effective GNN model aimed at performing the NA task even in networks without node attributes.

ACKNOWLEDGMENTS

This work was supported by the National Research Foundation of Korea (NRF) grant funded by the Korea government (MSIT) under Grants 2021R1A2C3004345 and RS-2023-00220762. An earlier version of this article was presented in part at the AAAI Conference on Artificial Intelligence, Virtual Event, February/March 2022 [39].

REFERENCES

- [1] S. Zhang and H. Tong, "FINAL: Fast attributed network alignment," in *Proc. 22nd ACM SIGKDD Int. Conf. Knowledge Discovery & Data Mining (KDD'16)*, San Francisco, CA, Aug. 2016, pp. 1345–1354.
- [2] H. T. Trung, T. Van Vinh, N. T. Tam, H. Yin, M. Weidlich, and N. Q. V. Hung, "Adaptive network alignment with unsupervised and multi-order convolutional networks," in *Proc. 36th Int. Conf. Data Eng. (ICDE'20)*, Dallas, TX, Apr. 2020, pp. 85–96.
- [3] F. Zhou, L. Liu, K. Zhang, G. Trajcevski, J. Wu, and T. Zhong, "DeepLink: A deep learning approach for user identity linkage," in *Proc. 37th IEEE Conf. Comput. Commun. (INFOCOM'18)*, Honolulu, HI, Apr. 2018, pp. 1313–1321.
- [4] X. Kong, J. Zhang, and P. S. Yu, "Inferring anchor links across multiple heterogeneous social networks," in *Proc. 22nd ACM Int. Conf. Inf. Knowl. Manage. (CIKM'13)*, New York, NY, Oct. 2013, pp. 179–188.
- [5] J. Ni, H. Tong, W. Fan, and X. Zhang, "Inside the atoms: ranking on a network of networks," in *Proc. 20th ACM SIGKDD Int. Conf. Knowledge Discovery & Data Mining (KDD'14)*, New York City, NY, Aug. 2014, pp. 1356–1365.
- [6] L. Liu, W. K. Cheung, X. Li, and L. Liao, "Aligning users across social networks using network embedding," in *Proc. 25th Int. Joint Conf. Artif. Intell. (IJCAI'16)*, New York City, NY, Jul. 2016, pp. 1774–1780.
- [7] T. Man, H. Shen, S. Liu, X. Jin, and X. Cheng, "Predict anchor links across social networks via an embedding approach," in *Proc. 25th Int. Joint Conf. Artif. Intell. (IJCAI'16)*, vol. 16, New York City, NY, Jul. 2016, pp. 1823–1829.
- [8] M. Heimann, H. Shen, T. Safavi, and D. Koutra, "REGAL: Representation learning-based graph alignment," in *Proc. 27th ACM Int. Conf. Inf. Knowl. Manage. (CIKM'18)*, Turin, Italy, Oct. 2018, pp. 117–126.
- [9] R. Singh, J. Xu, and B. Berger, "Global alignment of multiple protein interaction networks with application to functional orthology detection," *Nat. Acad. Sci.*, vol. 105, no. 35, pp. 12763–12768, 2008.
- [10] M. Bayati, M. Gerritsen, D. F. Gleich, A. Saberi, and Y. Wang, "Algorithms for large, sparse network alignment problems," in *Proc. 9th Int. Conf. Data Mining (ICDM'09)*, Miami Beach, FL, Dec. 2009, pp. 705–710.
- [11] E. Zhong, W. Fan, J. Wang, L. Xiao, and Y. Li, "ComSoc: adaptive transfer of user behaviors over composite social network," in *Proc. 18th ACM SIGKDD Int. Conf. Knowl. Discovery & Data Mining (KDD'12)*, Beijing, China, Aug. 2012, pp. 696–704.
- [12] A. Tversky, "Features of similarity," *Psychol. Rev.*, vol. 84, no. 4, pp. 327–352, 1977.
- [13] J. Zhang and S. Y. Philip, "Integrated anchor and social link predictions across social networks," in *Proc. 24th Int. Joint Conf. Artif. Intell. (IJCAI'15)*, Buenos Aires, Argentina, Jul. 2015, pp. 2125–2131.
- [14] D. Koutra, H. Tong, and D. Lubensky, "BIG-ALIGN: Fast bipartite graph alignment," in *Proc. IEEE 13th Int. Conf. Data Mining (ICDM'13)*, Dallas, TX, Dec. 2013, pp. 389–398.
- [15] J. Zhang, B. Chen, X. Wang, H. Chen, C. Li, F. Jin, G. Song, and Y. Zhang, "MEgo2Vec: Embedding matched ego networks for user alignment across social networks," in *Proc. 27th ACM Int. Conf. Inf. Knowl. Manage. (CIKM'18)*, Turin, Italy, Oct. 2018, pp. 327–336.
- [16] X. Mu, F. Zhu, E.-P. Lim, J. Xiao, J. Wang, and Z.-H. Zhou, "User identity linkage by latent user space modelling," in *Proc. 22th ACM SIGKDD Int. Conf. Knowledge Discovery & Data Mining (KDD'16)*, San Francisco, CA, Aug. 2016, pp. 1775–1784.
- [17] P. Cui, X. Wang, J. Pei, and W. Zhu, "A survey on network embedding," *IEEE Trans. Knowl. Data Eng.*, vol. 31, no. 5, pp. 833–852, May 2019.
- [18] T. Mikolov, I. Sutskever, K. Chen, G. S. Corrado, and J. Dean, "Distributed representations of words and phrases and their compositionality," in *Proc. 27th Conf. Neural Inf. Processing Systems (NIPS'13)*, Lake Tahoe, NV, Dec. 2013, pp. 3111–3119.
- [19] X. Du, J. Yan, and H. Zha, "Joint link prediction and network alignment via cross-graph embedding," in *Proc. 28th Int. Joint Conf. Artif. Intell. (IJCAI'19)*, Macao, China, Aug. 2019, pp. 2251–2257.
- [20] T. N. Kipf and M. Welling, "Semi-supervised classification with graph convolutional networks," in *Proc. 5th Int. Conf. Learning Rep. (ICLR'17)*, Toulon, France, Apr. 2017, pp. 1–14.
- [21] W. Hamilton, Z. Ying, and J. Leskovec, "Inductive representation learning on large graphs," in *Proc. 28th Int. Conf. Neural Inf. Process. Syst. (NIPS'17)*, Long Beach, CA, Dec. 2017, pp. 1024–1034.
- [22] K. Xu, W. Hu, J. Leskovec, and S. Jegelka, "How powerful are graph neural networks?" in *Proc. 7th Int. Conf. Learning Rep. (ICLR'19)*, New Orleans, LA, May 2019, pp. 1–17.
- [23] P. Velickovic, G. Cucurull, A. Casanova, A. Romero, P. Liò, and Y. Bengio, "Graph attention networks," in *Proc. 6th Int. Conf. on*

- Learning Rep.*, (ICLR'18), Vancouver, Canada, Apr./May 2018, pp. 1–12.
- [24] S. Tan, Z. Guan, D. Cai, X. Qin, J. Bu, and C. Chen, “Mapping users across networks by manifold alignment on hypergraph,” in *Proc. 28th AAAI Conf. on Artif. Intell. (AAAI'14)*, vol. 28, no. 1, Québec, Canada, Jul. 2014, pp. 159–165.
- [25] G. Kollias, S. Mohammadi, and A. Grama, “Network similarity decomposition (NSD): A fast and scalable approach to network alignment,” *IEEE Transactions on Knowledge and Data Engineering*, vol. 24, no. 12, pp. 2232–2243, 2011.
- [26] J. Gilmer, S. S. Schoenholz, P. F. Riley, O. Vinyals, and G. E. Dahl, “Neural message passing for quantum chemistry,” in *Proc. 34th Int. Conf. Mach. Learn. (ICML'17)*, Sydney, Australia, Aug 2017, pp. 1263–1272.
- [27] B. D. McKay and A. Piperno, “Practical graph isomorphism, ii,” *J. Symbolic Comput.*, vol. 60, pp. 94–112, Jan. 2014.
- [28] J. Zhou, G. Cui, S. Hu, Z. Zhang, C. Yang, Z. Liu, L. Wang, C. Li, and M. Sun, “Graph neural networks: A review of methods and applications,” *AI Open*, vol. 1, pp. 57–81, 2020.
- [29] Z. Zhang, P. Cui, and W. Zhu, “Deep learning on graphs: A survey,” *IEEE Trans. Knowl. Data Eng.*, vol. 34, no. 1, pp. 249–270, Jan. 2022.
- [30] Z. Wu, S. Pan, F. Chen, G. Long, C. Zhang, and S. Y. Philip, “A comprehensive survey on graph neural networks,” *IEEE Trans. Neural Netw. Learn. Syst.*, vol. 32, no. 1, pp. 4–24, Mar. 2020.
- [31] X. Cao and Y. Yu, “BASS: A bootstrapping approach for aligning heterogenous social networks,” in *Proc. Joint Eur. Conf. Mach. Learn. Knowl. Discovery Databases (ECML-PKDD'16)*, 2016, pp. 459–475.
- [32] R. Rossi and N. Ahmed, “The network data repository with interactive graph analytics and visualization,” in *Proc. 29th AAAI Conf. on Artif. Intell. (AAAI'15)*, Austin, Texas, Jan. 2015.
- [33] A. Prado, M. Plantevit, C. Robardet, and J.-F. Boulicaut, “Mining graph topological patterns: Finding covariations among vertex descriptors,” *IEEE Trans. Knowl. Data Eng.*, vol. 25, no. 9, pp. 2090–2104, Sept. 2013.
- [34] B. Perozzi, R. Al-Rfou, and S. Skiena, “DeepWalk: Online learning of social representations,” in *Proc. 20th ACM SIGKDD Int. Conf. Knowledge Discovery & Data Mining (KDD'14)*, New York City, NY, Aug. 2014, pp. 701–710.
- [35] M. Fey and J. E. Lenssen, “Fast graph representation learning with pytorch geometric,” in *Proc. ICLR Workshop on Representation Learning on Graphs and Manifolds*, New Orleans, LA, May 2019, pp. 1–9.
- [36] D. P. Kingma and J. Ba, “Adam: A method for stochastic optimization,” in *Proc. 3rd Int. Conf. Learn. Representations (ICLR'15)*, San Diego, CA, May 2015, pp. 1–15.
- [37] V. Nair and G. E. Hinton, “Rectified linear units improve restricted Boltzmann machines,” in *Proc. 27th Int. Conf. Mach. Learn. (ICML'10)*, Haifa, Israel, Jun. 2010, pp. 807–814.
- [38] D. Chen, Y. Lin, W. Li, P. Li, J. Zhou, and X. Sun, “Measuring and relieving the over-smoothing problem for graph neural networks from the topological view,” in *Proc. 34th AAAI Conf. on Artif. Intell. (AAAI'20)*, vol. 34, no. 04, New York City, NY, Feb 2020, pp. 3438–3445.
- [39] J.-D. Park, C. Tran, W.-Y. Shin, and X. Cao, “Grad-Align: Gradual network alignment via graph neural networks (Student Abstract),” in *Proc. 36th AAAI Conf. on Artif. Intell. (AAAI'22)*, Virtual Event, Feb. 2022.